

Investigation of a Catalyst Ink Dispersion Using Both Ultra-Small-Angle X-ray Scattering and Cryogenic TEM

Fan Xu,[†] HangYu Zhang,[§] Jan Ilavsky,[⊥] Lia Stanciu,^{§,||} Derek Ho,[#] Matthew J. Justice,[‡] Horia I. Petrache,[‡] and Jian Xie*,[†]

[†]Department of Mechanical Engineering, [‡]Department of Physics, Indiana University—Purdue University Indianapolis (IUPUI), Indianapolis, Indiana 46202, United States, [§]Weldon School of Biomedical Engineering, and ^{||}School of Materials Engineering, Purdue University, West Lafayette, Indiana 47907, United States,

[⊥]X-ray Science Division, Argonne National Laboratory, Argonne, Illinois 60439, United States, and

[#]Polymer Division, National Institute of Standards and Technology, Gaithersburg, Maryland 20899-8562, United States

Received July 15, 2010. Revised Manuscript Received October 13, 2010

The dispersion of Nafion ionomer particles and Pt/C catalyst aggregates in liquid media was studied using both ultra-small-angle X-ray scattering (USAXS) and cryogenic TEM. A systematic approach was taken to study first the dispersion of each component (i.e., ionomer particles and Pt/C aggregates), then the combination of the components, and last the catalyst ink. Multiple-level curve fitting was used to extract the particle size, size distribution, and geometry of the Pt/C aggregates and the Nafion particles in liquid media from the scattering data. The results suggest that the particle size, size distribution, and geometry are not uniform throughout the systems but rather vary significantly. It was found that the interaction of each component (i.e., the Nafion ionomer particles and the Pt/C aggregates) occurs in the dispersion. Cryogenic TEM was used to observe the size and geometry of the particles in liquid directly and to validate the scattering results. The TEM results showed excellent agreement.

1. Introduction

With the increasing environmental requirements of reducing automobile emissions, the polymer electrolyte fuel cell (PEFC) has received increasing amounts of attention as one of the best candidates for the hydrogen economy not only because it has zero emission but also because it has a higher energy efficiency (i.e., > 65%) than does the internal combustion engine. The membrane electrode assembly (MEA) is the core component of the PEFC, where the fuel, hydrogen, is directly electrochemically converted into electricity. The MEA determines not only the performance of the PEFC but also the cost. Hence, developing a high-performance, low-cost durable MEA is critical for accelerating the commercialization of PEFCs.

A typical MEA is a composite of a polymer electrolyte membrane that is sandwiched between two porous catalyst layers (as schematically shown in Figure 1 in the Supporting Information). The catalyst layers consist of a network of recast Nafion ionomer that holds carbon aggregates together. The precious metal catalyst nanoparticles are attached to the surface of the carbon aggregates. To achieve maximum performance, the catalyst layer needs to have (i) the maximum interface of Nafion/catalyst for both anode and cathode gas reactions, (ii) the appropriate pore structure to allow gas diffusion and water dissipation, and (iii) optimized Nafion networks that bind the carbon aggregates together, provide structural integrity for the catalyst layer, and provide a proton conduction path. Numerous new techniques for the fabrication of catalyst layers/MEAs have been explored, such as doctor-blade spreading, electrophoretic deposition (EPD), sputtering, electrospraying, and rolling.^{1–4}

Among all of the different techniques for MEA and catalyst layer fabrication, a method developed at Los Alamos National Laboratory (LANL) using the “thin film decal” process^{5,6} is still widely used today in the development of both hydrogen and direct methanol fuel cells. In this process, a Pt/C catalyst powder is dispersed in a solvent (i.e., water or an organic solvent such as glycerol) with an ionomer suspension (generally a 5 wt % Nafion solution) to form a uniform suspension, a catalyst ink. Then, this catalyst ink is painted onto Teflon-coated fiberglass substrates (the decal), which are then heat treated to remove the solvents and form a porous solid catalyst layer. The formed catalyst layer decals are then hot pressed onto both sides of a Nafion membrane to form the MEA. Despite numerous modifications over time, the basic technique has remained essentially the same: disperse the catalyst powder and Nafion ionomer particles in a liquid media first, and then form a porous solid catalyst layer. The catalyst layer formation process is, basically, a condensation process of catalyst ink as shown in Figure 1. Obviously, the structure of the formed solid catalyst layer depends on (1) the dispersion of the Pt/C aggregates and the ionomer particles in the catalyst ink and (2) the evaporation of the solvent in the catalyst ink to form the porous solid catalyst layer (the condensation of the catalyst ink).

The dispersion of the Pt/C aggregates and the ionomer particles inside the solvent is the first step in making the catalyst layer structure solid. To have an appropriate ink system, the Pt/C catalyst powder must be well dispersed and form small aggregates (on a 100 nm scale) and the ionomer particles must form small-diameter strips or rods so that they can bind the Pt/C aggregates together in the solid layer. All of the nanoscale catalyst particles should come into contact uniformly with the other components (the ionomer and the carbon aggregates) to form a porous, rigid

*Corresponding author. E-mail: jianxie@iupui.edu.

(1) Aldebert, P.; Novel-Cattin, F.; Pineri, M.; Durand, R. *Solid State Ionics* **1989**, *35*, 3.

(2) Talyor, E. J.; Anderson, E. B.; Vilambi, N. R. K. *J. Electrochem. Soc.* **1992**, *139*, 45.

(3) Hirano, S.; Kim, J.; Srinivasan, S. *Electrochim. Acta* **1997**, *42*, 1587.

(4) Amine, K.; Yasuda, K.; Takenaka, H. *Ann. Chim. Sci. Mater.* **1998**, *23*, 331.

(5) Wilson, M. S.; Gottesfeld, S. *J. Electrochem. Soc.* **1992**, *139*, 28.

(6) Wilson, M. S.; Gottesfeld, S. *J. Appl. Electrochem.* **1992**, *22*, 1.

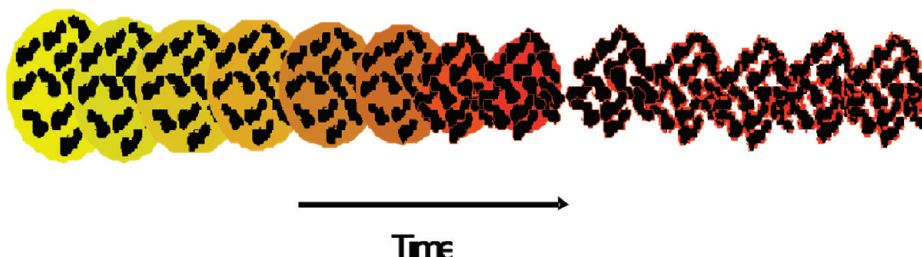


Figure 1. Schematic of the agglomeration of the Pt/C aggregates in a catalyst ink during the solvent evaporation process.

solid catalyst layer/MEA, which will lead to better performance. The optimization of a catalyst ink with different components and solvents is called ink formulation and is a critical step in manufacturing a high-performance MEA. Because of this critical step, it is of great importance to verify whether a formulated catalyst ink disperses the Pt/C aggregates and the ionomer particles well. The current approach has been to use different ink formulations with the various preparation protocols for the MEAs and then to measure the MEA fuel cell performance to verify the ink formulation. This is a typical trial-and-error approach that often provides little fundamental understanding of the ink system in terms of its particle size, size distribution, and geometry and how they are associated with the performance of the catalyst layer/MEA. Another is a rational approach that first designs an “ideal” catalyst layer structure based on the need for gas diffusion, proton conduction, and water transport guided by modeling and then develops a catalyst ink with the desired dispersion of Pt/C aggregates and ionomer particles. To use this rational approach, a technique is needed to study the size and geometry of both the Pt/C aggregates and the ionomer particles in catalyst inks and the effects of the solvents and other components on the Pt/C and ionomer dispersion. Therefore, to verify the “optimized” ink formulation and make a rationally designed, high-performance catalyst layer MEA, it is critical to develop an effective way to systematically measure the detailed organization of the microstructure (particle size and geometry) of the catalyst/carbon aggregates and the Nafion ionomer in catalyst inks.

Some research^{7–13} has been conducted to investigate the microstructure of Nafion solutions using dynamic light scattering (DLS),^{7,8} small-angle X-ray scattering (SAXS, with a Nafion concentration ranging from 5 to 20 wt %),¹² and electron spin resonance (ESR, with a Nafion concentration ranging from 1 to 22 wt %).¹⁴ In most of the literature,^{9–11,13} the compact cylinder model was used to fit the SAXS and the small angle neutron scattering (SANS) data. It was also found that the solvent and polymer contact was at the surface of the micelle. This result is different from the result of the open-coil model fitting, which suggests that the solvent–polymer contact is maintained all along the chain. Gebel¹² and Loppinet et al.¹³ indicated from the SAXS results that the Nafion ionomer is a rodlike structure with $d = 2.5$ nm and $L = 17$ nm. So far, the microstructure of Nafion in liquid media has been reported only from the curve fittings of the scattering data; no direct observation has been reported to validate these scattering results.

Furthermore, there have not yet been any publications about the detailed microstructure of the Nafion ionomer and the Pt/C in a catalyst ink. The main challenge in catalyst ink research arises from the strong absorption of visible and UV light by the ink (Pt/C carbon aggregates). It was found in our previous work that the DLS technique responds only to highly diluted ink, which could lead to a deviation from the original dispersion. Neutron and X-ray scattering can overcome this absorption problem of determining the size and geometry of Nafion ionomer particles and Pt/C aggregates in liquid media because they both have a high-energy incident beam so the absorption of the beam by the Pt/C aggregates in a catalyst ink can be effectively eliminated.

Here we present our work on developing an effective method to study the microgeometry, particle size, and interactions of carbon, the Nafion ionomer, and solvents in inks using ultra-small-angle X-ray scattering (USAXS) with direct observation using cryogenic transmission electron microscopy (cryo-TEM). A systematic approach was taken to study (i) the individual components of the ionomer particles and the Pt/C aggregate dispersion in the solvents alone, (ii) the separate combinations of the components (i.e., ionomer particles + TBAOH, ionomer particles + TBAOH + Pt/C aggregates), and (iii) a combination of all of the components in the real catalyst inks. This approach follows the steps in the ink-preparation process (schematically shown in Figure 2 in the Supporting Information) and provides the particle size and geometry in the system during that process. We also demonstrate that this novel and systematic approach can reveal both the dispersion of the Pt/C and Nafion particles in catalyst inks and the interaction of the Pt/C and Nafion particles in liquid media.

2. Experimental Section

Materials and Catalyst Ink Preparation. Catalyst inks were prepared by mixing the carbon-supported catalyst (i.e., 20% Pt/C, BASF-ETEK) with a 5% Nafion solution (1100 EW, Solution Technologies, Inc.), 1.0 M tetrabutylammonium hydroxide (TBAOH), and glycerol (Fisher Scientific). The inks were ultrasonicated for 30 min and stirred vigorously overnight to achieve a uniform suspension. The sample information is listed in Table 1.

TEM Analysis. The 5% Nafion solution was diluted by isopropanol and water (4:1) to 0.1%. The low-concentration Nafion solution (0.1%) was used to observe the Nafion particle geometry. The use of such a low concentration of Nafion solution was to prevent the Nafion particles from agglomerating when a drop of the solution was dried on a TEM grid. The morphologies of the Nafion ionomer and the commercial catalyst samples were examined using a Philip Tecnai 20 transmission electron microscope (TEM). All of the measurements were repeated for at least three samples to ensure data reproducibility.

Cryogenic Temperature TEM Analysis. To get a clear image of the Nafion ionomer particles, a special 5% Nafion solution in Ce³⁺ form was used for the cryo-TEM analysis. This was done by mixing 0.2 M Ce₂(SO₄)₃ and the 5% Nafion solution to replace the H⁺ in Nafion with Ce³⁺. To remove the excess Ce³⁺ in the exchanged Nafion solution, the solution was heated to form

- (7) Cirkel, P. A.; Okada, T.; Kinugasa, S. *Macromolecules* **1999**, *32*, 531.
- (8) Jiang, S.; Xia, K. Q.; Xu, G. *Macromolecules* **2001**, *34*, 7783.
- (9) Pietek, E. S.; Schlick, S. *Langmuir* **1994**, *10*, 2188.
- (10) Alderbert, P.; Dreyfus, B.; Pineri, M. *Macromolecules* **1986**, *19*, 2651.
- (11) Li, H.; Schlick, S. *Polymer* **1995**, *36*, 1141.
- (12) Gebel, G. *Polymer* **2000**, *41*, 15, 5829.
- (13) Loppinet, B.; Gebel, G.; Williams, C. E. *J Phys Chem B* **1997**, *101*, 1884.
- (14) Lee, S. J.; Yua, T. L.; Lina, H. L.; Liu, W. H.; Lai, C. L. *Polymer* **2004**, *45*, 2853.

Table 1. Sample Preparation for USAXS Measurements

sample	Nafion (g)	glycerol/d8-G ^a (g)	TBAOH (g)	Pt/C (g)
Nafion	1	0	0	0
Nafion + G ^a	1	1	0	0
Nafion + G ^a + T ^b	1.034	1.034	0.052	0
28% Pt/C + G ^a	0	2.74	0	0.35
28% Nafion + Pt/G	2.185	0	0	0.28
28% Nafion + T ^b + Pt/C	2.185	0	0.11	0.28
28% Nafion + Pt/C + G	2.185	2.185	0	0.28
28% Nafion ink ^c	1.034	1.034	0.052	0.13

^aG: glycerol. ^bT: tetrabutylammonium hydroxide (TBAOH). ^cink: Pt/C aggregates + Nafion + TBAOH + glycerol.

a milky white gel and then washed using DI water at least six times. Finally, the milky white gel was dissolved using the mixture of isopropanol, *n*-propanol, methanol, and water to form a uniform suspension.

A 3.5 μL aliquot of the Nafion sample was placed on a copper grid (400 mesh) coated with a holey carbon film. The excess sample was blotted off with filter paper. The grid was then immediately plunged into liquid ethane cooled by liquid N₂. The sample grid was loaded into the microscope with a Gatan side-entry cryoholder. Low-dose images were collected using a CM200 or CM300 cryomicroscope with a field emission gun operating at 200 or 300 kV, respectively.

USAXS Measurements. USAXS measurements were conducted with the versatile USAXS instrument at the Advanced Photon Source (APS), Argonne National Laboratory. The USAXS has angular and energy resolutions of the order of 10⁻⁴, accurate and repeatable X-ray energy tunability over its operational energy range from 8 to 18 keV, a dynamic intensity range of 10⁸ to 10⁹, and a scattering vector range of 0.0001 to 1 \AA^{-1} .

3. Methods

Global Unified Fitting.^{15–17} The scattering data were described by global unified fit analysis employing Porod and Guinier scattering regimes as described here. At large scattering angles, high values of the momentum transfer vector, *q*, can be obtained, which reflect a small size, *d*, obtained by Bragg's law:

$$d = \frac{2\pi}{q} \quad (1)$$

At a high *q*, *I*(*q*) (the scattering intensity) follows Porod's law

$$I(q) = Bq^{-4}, \text{ where } B = 2\pi N(\Delta\rho)2S \quad (2)$$

where *S* is the average surface area of a particle, *N* is the number density of primary particles in the measured scattering volume, and $\Delta\rho$ is the difference in electron density between the background of the solvent and the particles.

From higher *q* to lower *q*, the linear power law (Porod) regime, whose slope gives geometric information, is followed by a kneelike Guinier regime that reflects the structural size of the primary particles. Equation 3 is Guinier's law for the kneelike regimes,

$$I(q) = G_i \exp(-q^2 R_{gi}^{2/3}) \text{ where } G_i = N_i(\Delta\rho)2\nu_i^2 \quad (3)$$

Here, *G_i* is the exponential prefactor, *N_i* and ν_i are the number density and the volume of a primary particle in the Guinier regime, respectively, and *i* is the number of fitting levels. If there are agglomerate particles in the system, then *i* would be higher than 1. Furthermore, the radius of gyration of the primary particles, $R_g(D_g/2)$, can be obtained from eq 3.

If there are agglomerate particles in the system, then there would be several Guinier knees. The slope of the power law

between two Guinier knees is directly related to the mass fractal structure of the agglomerates by eq 4

$$I(q) = B_f q^{-D_f} \quad (4)$$

where *D_f* is the mass fractal dimension and *B_f* is a power law prefactor,

$$B_f = \left(\frac{G_f D_f}{R_{gi}^{D_f}} \right) \Gamma D_f^{f/2} \quad (5)$$

G_f is a constant defined by eq 3, and Γ is the gamma function.

Unified global fitting provides for as many as five independent levels (*n* = 5), including the structure factor^{15,17} (interparticle interference):

$$I(q) = F_B + \sum_{i=1}^n S_i(Q) \left(G_i \exp\left(-\frac{Q^2 R_{gi}}{3}\right) + B_i \exp\left(-\frac{Q^2 R_{gef_i}}{3}\right) \times \left\{ \frac{\operatorname{erf}\left(\frac{QR_{gi}}{6^{1/2}}\right)^3}{Q} \right\}^{P_i} \right) \quad (6)$$

Here, *F_B* is an optional flat background and *B_i* is the same as *B_f* mentioned before (a constant prefactor), specific to the type of power-law scattering, *P_i*.

Particle Size Distribution.¹⁶ The USAXS curves were analyzed by comparing them with scattering model functions implemented in an Igor Pro-based software package. The Irena size-distribution tool was used with the maximum entropy (MaxEnt) method to evaluate the size distribution from the USAXS data.

The curve was separated into several levels, depending on the different sample systems, from high *q* to low *q* according to the unified global fitting. In the ink system, spheroid and cylinder models were employed separately in different fitting levels to analyze the particle size distribution. Different regions were analyzed by the MaxEnt size distribution function with the Igor Pro software, resulting in a particle volume distribution ($\text{cm}^3 \cdot \text{cm}^{-3} \cdot \text{\AA}^{-1}$) versus scattering diameters (\AA). After this step, a normalization calculation was carried out using eq 7:

$$\text{percentage of particle} = \frac{\text{particle volume}}{\sum \text{particle volume}} \times 100\% \quad (7)$$

After normalization, the percentage of the particle (%) versus the scattering diameter (nm) was obtained. The size distributions for all of the ranges were combined to show the total particle size distribution.

4. Results and Discussion

The size and microgeometry of all samples were derived from the USAXS data using curve fitting. To validate the results from the USAXS data further, all samples were analyzed using cryogenic TEM to provide a direct observation of the particle size and microgeometry. The advantage of cryogenic TEM is that

(15) Kammler, H. K.; Beaucage, G.; Mueller, R.; Pratsinis, S. E. *Langmuir* **2004**, 20, 1915.

(16) Ilavsky, J.; Jemian, P. R. *J. Appl. Crystallogr.* **2009**, 42, 347.

(17) Beaucage, G. *Phys. Rev.* **2004**, 70, 1401.

Table 2. Summary of the Geometry and Particle Size of the USAXS Measurement Fitting Results and Cryo-TEM Results

sample	USAXS	cryo-TEM
Nafion	rod: length = 21.4 ± 1.4 nm $D = 3 \pm 0.2$ nm	rod: length = $\sim 20 - 30$ nm $D = \sim 3$ to 4 nm
Nafion + G ^a	rod: length = 14 ± 1.4 nm $D = 2.4 \pm 0.2$ nm	
Nafion + G + T ^b	rod: length = $33.3 - 48.7$ nm $D = 5 \pm 0.2$ nm	
28% Pt/C + G	sphere: $D = 46.8$ nm sphere: $D = 62 \pm 5$ nm rod: length = 520 ± 20 nm $D = 60 \pm 5$ nm primary particle size = ~ 80 nm rod: $D = 3.9 \pm 0.2$ nm sphere: $D = 66 \pm 1.4$ nm rod: length = 102.7 ± 5 nm $D = 60 \pm 2$ nm agglomerated particle: $D = 292.3 \pm 5$ nm primary particle diameter = $60 - 100$ nm rod: $D = 3.6 \pm 0.2$ nm sphere: $D = 64 \pm 2$ nm rod: length = 201.7 ± 5 nm, $D = 64 \pm 2$ nm agglomerated particle length > 300 nm primary particle size = $\sim 120 - 200$ nm rod: $D = 3.2 \pm 0.2$ nm sphere: $D = 54 \pm 2$ nm rod: length = 159.7 ± 10 nm $D = 30$ nm rod: length = 290 ± 10 nm width = 90 nm primary particle = 90 nm rod: $D = 3.28 \pm 0.2$ nm sphere: $D = 47.4 \pm 2.5$ nm rod: length = 169.8 ± 10 nm rod: length > 290 ± 10 nm primary particle = $100 - 200$ nm	sphere (carbon): $D = \sim 20 - 60$ nm sphere (carbon): $D = 50 - 80$ nm rod (aggregated carbon particles): length = ~ 400 nm $D = \sim 60$ nm primary particle size = ~ 60 nm rod (Nafion ionomer): $D = 4.2$ nm sphere (carbon): 70 ± 5 nm rod (aggregated carbon particles): length = $\sim 150 \pm 10$ nm $D = 60 \pm 2$ nm l-like agglomerated particle: length = ~ 200 nm primary particle diameter = $70 - 100$ nm
28% Nafion + Pt/C		sphere (carbon): $D = \sim 70$ nm rod (aggregated carbon particles): length = ~ 210 nm agglomerated particle length = ~ 420 nm primary particle size = ~ 200 nm
28% Nafion + T ^b + Pt/C		sphere (carbon): $D = \sim 80 - 130$ nm rod (aggregated carbon particles): length = ~ 350 nm $D = \sim 90$ nm agglomerated particle length > ~ 500 nm primary particle size = ~ 80 nm sphere (carbon): $D = \sim 50$ nm rod (aggregated carbon particles): length = 250 ± 10 nm width = 200 ± 10 nm agglomerated particle length > ~ 500 nm primary particle = $100 - 200$ nm
28% Pt/C + Nafion + G		
28% Nafion ink ^c		

^aG: glycerol. ^bT: tetrabutylammonium hydroxide (TBAOH). ^cInk: Pt/C aggregates + Nafion + TBAOH + glycerol.

the morphology of the particles in a liquid can be directly observed without disturbing them. This can be achieved by fast freezing the samples to lock their original particle structure in the liquid media. The combination of USAXS and cryogenic TEM measurements can provide the real microstructures of the catalyst and Nafion particles in the liquid media. The scattering data of the different systems in this study showed the variation of the slope over the whole q range, suggesting that the particles have nonuniform sizes and different geometries. Multilevel fitting was employed, and the results indicate that each system may have had a different particle size and geometry. The fitting results confirmed by cryo-TEM images are summarized in Table 2 for the different systems.

Nafion Ionomer in Liquid Media. The dispersion of the Nafion particles in the liquid was studied first. Two different approaches were carried out to obtain in situ geometry information on the Nafion ionomer particles in the Nafion solution: the first was TEM of a very dilute Nafion solution (0.1%), and the second was cryo-TEM of the 5% Ce³⁺-formed Nafion solution. The images are shown in Figure 2. The 5% Nafion solution was diluted by isopropanol and water (4:1) to 0.1% so that the Nafion ionomer particles would not agglomerate. A drop of this liquid was placed onto the TEM grid, the liquid was fast frozen, and a cryogenic TEM image was taken. The TEM image of the 0.1% Nafion solution is shown in Figure 2a, where the Nafion ionomer in the isopropanol is a rodlike particle that is $\sim 20 - 30$ nm in length and $\sim 2 - 3$ nm in diameter. This value is very close to that reported by Gebel et al.¹² for a Nafion ionomer in a dilute solution (cylinder, $D = 2.5$ nm, $L = 17$ nm). As for the 5% Nafion ionomer

in Ce³⁺ form, the cryo-TEM image is shown in Figure 2b: the black rodlike particle is the SO₃²⁻ group with Ce³⁺, where it can easily be seen that the rodlike particle is the Nafion ionomer. The size of the single Nafion thread ionomer was almost the same as that in the 0.1% Nafion solution. The diameter of the Ce³⁺ Nafion ionomer was $\sim 3 - 4$ nm, the length was $\sim 20 - 30$ nm.

The typical scattering data obtained from USAXS measurements of a 5% Nafion solution is shown in Figure 3. There was a decrease in intensity at low q and a peak at medium q , which is ascribed to the long-range crystalline domains of the lamellar structure of the Nafion ionomer in the polymer matrix.¹⁸ The signal of the high- q region was too weak for reliable data evaluation and was not considered in the following discussion. Scattering data (black circles) were fit using the global unified function (red solid line). A power law of -2 (slope) (green dashed line, Porod fit; Figure 3a) was observed for the primary particles and reflects soft agglomerated primary particles that are consistent with the TEM inset. This power-law (Porod) regime was followed at lower q (~ 0.07 Å⁻¹) by a kneelike decay (Guinier) regime (blue dotted line, Guinier fit). This kneelike decay in intensity reflects the structural size of the primary particles. The dip in the intensity at low q indicates the presence of a structural factor. We chose to use the structural factor defined in the unified fit publications^{15,17} and implemented in the Irena package,¹⁶ which is usually suitable for complicated systems with relatively small corrections. As for Figure 3, the fitting result yielded that $D_g = \sim 3 \pm 0.2$ nm and the ETA (average interparticle distance)

(18) McLean, R. S.; Doyle, M.; Sauer, B. B. *Macromolecules* **2000**, *33*, 6541.

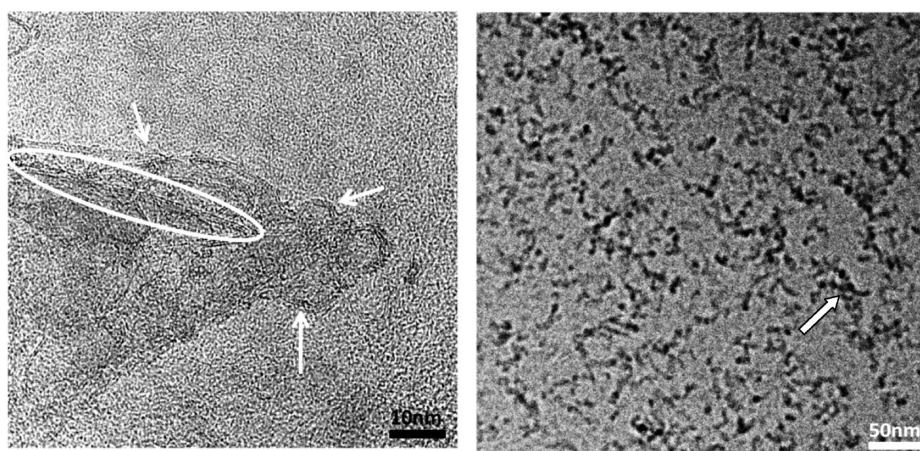


Figure 2. (Left) TEM of 0.1% very dilute Nafion solution (5% Nafion solution was diluted by isopropyl and water (4:1) to 0.1%). (Right) Cryo-TEM image of 5% Ce^{3+} from Nafion solution.

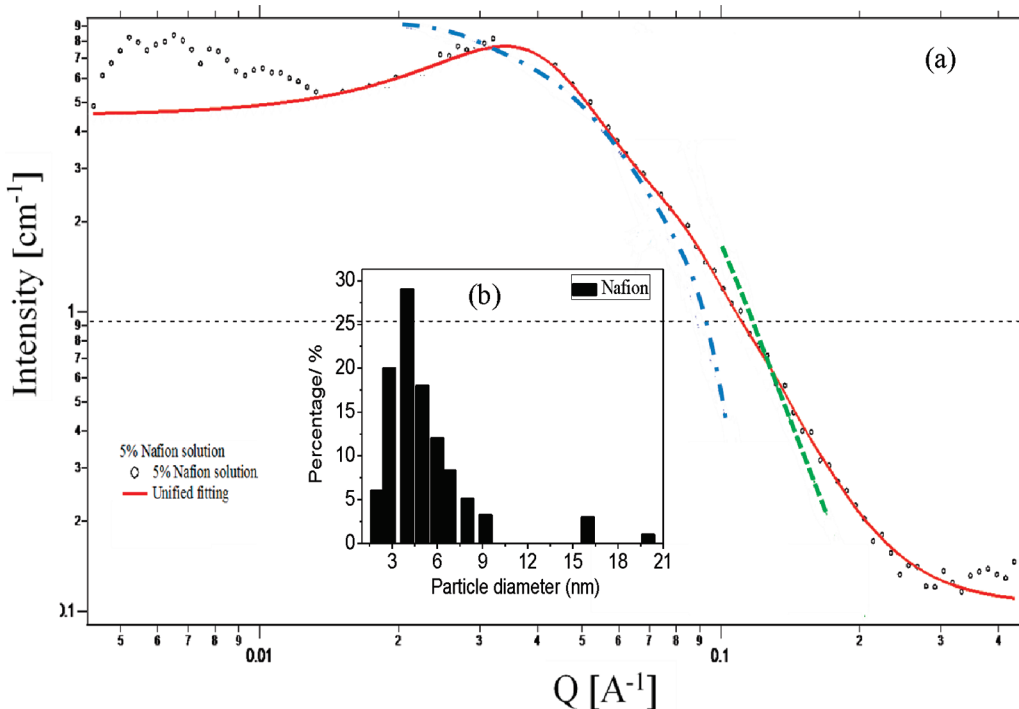


Figure 3. (a) USAXS pattern of a 5% Nafion solution (power law). The scattering data (circles) are well described by the global unified fit equation (solid line). Furthermore, one Porod regime (dashed line) is shown together with one Guinier regime (dotted line). (b) Particle size distribution;

was $\sim 14.1 \text{ nm}$, which is bit large for the 3 nm particles (diameter) so it can be assumed that these particles repelled each other. The fitting results agreed with the TEM images in Figure 2 and with Gebel's result.¹² Two aggregation processes were observed in Lee¹⁴ et al.'s experiment by membrane osmometry, viscoelasticity analysis, and dynamic light scattering. The authors attributed the primary aggregation process, which forms smaller (diameter = 10^3 nm) rodlike aggregated particles, to the hydrophobic interaction of the fluorocarbon backbone. The ionic aggregation of the primary aggregation particles that came from the electrostatic attraction of the Nafion side chain, SO_3^{2-} ion pairs, caused the secondary aggregation process, which formed larger aggregated particles (diameter = 10^4 nm). The Nafion ionomer particle sizes in their study were much larger than those in our observation (diameter = $3\text{--}14 \text{ nm}$). This is because Lee et al. used a much higher concentration Nafion solution than 0.5%. Assuming the

geometry of Nafion ionomer particles as a cylinder with a length of 15 nm , the particle size distribution (Figure 3b) was obtained using the Irena software package.¹⁶ The primary particle size for the Nafion solution was around $4\text{--}6 \text{ nm}$; however, there were a few particles between 15 and 20 nm , as indicated by the size distribution analysis.

The USAXS patterns of three different samples (Nafion ionomer, Nafion ionomer + glycerol, and Nafion ionomer + TBAOH + glycerol) are presented in Figure 4. Because glycerol serves as only a solvent and does not change the chemical structure of the Nafion ionomer, the local scattering regimes of the Nafion ionomer and the Nafion ionomer + glycerol almost overlapped in the region of $q = 0.1\text{--}1 \text{ \AA}^{-1}$. The unified global fitting showed that the Porod slopes were -2.06 and -1.4 and the rodlike structure was $D = 3 \pm 0.2$ and $2.4 \pm 0.2 \text{ nm}$. The Nafion ionomer and the Nafion ionomer + glycerol were $L = 21.4 \pm 1.4$

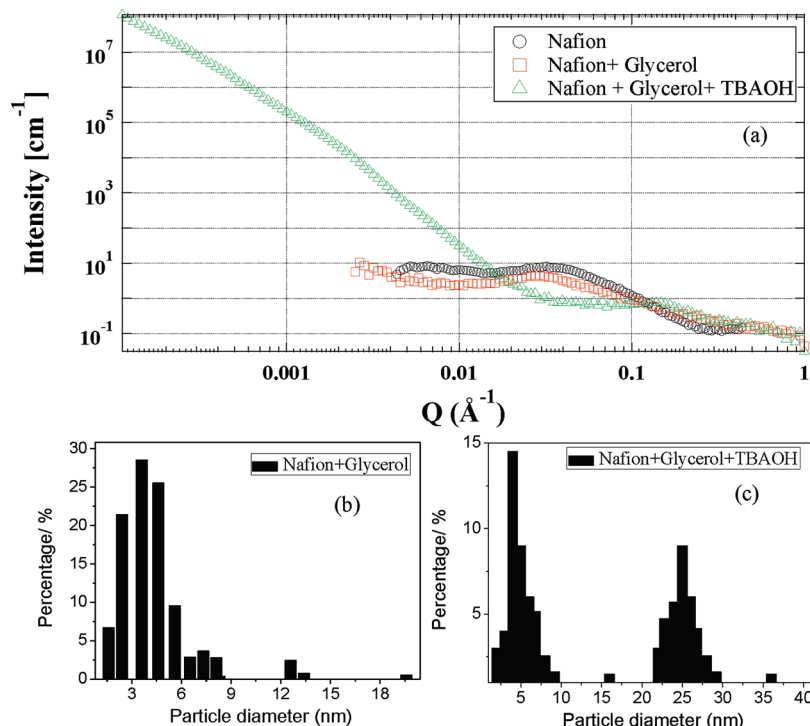


Figure 4. Comparison of the Nafion ionomer in different solvents. (a) USAXS plots of a 5% Nafion solution (triangles), Nafion + glycerol (squares), and Nafion + glycerol + TBAOH (circles). (b) Particle size distribution of Nafion + glycerol. (c) Particle size distribution of Nafion + glycerol + TBAOH.

and 14 ± 1.4 nm, respectively. When TBAOH was added to the system of the Nafion ionomer + glycerol, the high- q part (first power law slope of -2) of the scattering curve was almost the same as those of the Nafion ionomer and the Nafion ionomer + glycerol. However, remarkable differences appeared in the medium- and low- q regions, where the peak in medium q (from 0.01 to 0.1 \AA^{-1}) disappeared. In the low- q part (from 0.0001 to 0.01 \AA^{-1}), the second Porod regime appeared (slope -2.6), followed by a second Guinier regime, which suggests larger particles in the system. This may have been caused by the TBA⁺ (whose diameter is much larger than H⁺) replacing the H⁺ in the Nafion ionomer, which would make the Nafion ionomer particle size larger. The fitting results obtained by the global unified function are shown in Table 2, and there were particles with diameters of ~ 33.3 – 48.7 nm. The particle size distribution (by the cylinder model and the MaxEnt method with a length of 15 nm) is shown in Figure 4 as well. The Nafion + glycerol solution had a normal distribution (~ 3 to 4 nm), and Nafion + glycerol + TBAOH had a bimodal distribution (~ 3 to 4 and ~ 25 nm).

Pt/C Aggregates in Liquid Media. The Pt/C system was also investigated by USAXS and cryo-TEM to gain information about the geometry and particle size of the catalyst powder in liquid media. The catalyst system was more complex than the Nafion ionomer system in terms of size and geometry.

The USAXS data of the Pt/C catalyst powder in a glycerol solvent is shown in Figure 5. The solvent had a significant effect on the geometry and particle size of the Pt/C, as indicated by three distinctive regions with different slopes in Figure 5. Three-level fittings ($n = 3$) were used in the fitting of the scattering data of the Pt/C + glycerol system. The MaxEnt method was used in all levels of analysis. The spheroid model was employed in the first and second levels, and a cylinder model was used in the third level, according to the unified global fitting. The unified global fitting was used for the first-level fitting. The unified global fitting function results showed that in the first fitting level D_{g_1} was

19.4 ± 1 nm and the power-law slope P_1 was 2 . This level can be attributed to the size distribution of spherical particles. The cryo-TEM image in Figure 5c, which corresponds to the high- q area in Figure 5, reveals that the carbon black particles had spherical geometry (diameter = ~ 20 – 60 nm). As can be seen from the 800-nm-scale TEM image (Figure 5d), the percentage of this particle size increased from the Pt/C + Nafion system (Figure 7) to the Pt/C + glycerol system. More detailed information can be obtained from the full-range particle size distribution. The results of the particle size distribution analysis clearly showed the effects of the solvent on the Pt/C dispersion because the majority of the Nafion solution was isopropanol, which has a low viscosity whereas glycerol has a high viscosity. The second fitting level was $D_{g_2} = 62 \pm 5$ nm with a power-law slope of $P_2 = 2.93$. As can be seen from the cryo-TEM image (Figure 5d) that corresponds to this medium- q region, larger-sphere carbon particles, with a diameter of around 50 – 80 nm, were found. The aggregation of the Pt/C particles could not be totally avoided. The third-level fitting was $D_{g_3} = 520 \pm 20$ nm with a power-law slope of $P_3 = 4.32$. This scattering is likely attributed to the system of rodlike particles (aggregated by the Pt/C particles), as can be seen from the cryo-TEM image (Figure 5e). On the basis of the full-range particle size distribution in Figure 5, the primary particle size was about 80 nm, which agrees with the TEM results. As can be seen in the overview cryo-TEM (400 nm scale) image (Figure 5b), the primary particle size was around 60 nm. Overall, the Pt/C catalyst powder dispersed in glycerol had different particle sizes and geometries from those in the Nafion solution.

Pt/Carbon Black + Nafion System. This system is a typical example of the introduction of a unified global fitting. The slope of this system varied for the whole q range (Figure 6a), suggesting that the system is nonuniform in terms of particle size and geometry. This was also confirmed by the particle size distribution in Figure 6 and the cryo-TEM image (Figure 6a). Thus, a multilevel fitting was needed to analyze the scattering data. Four

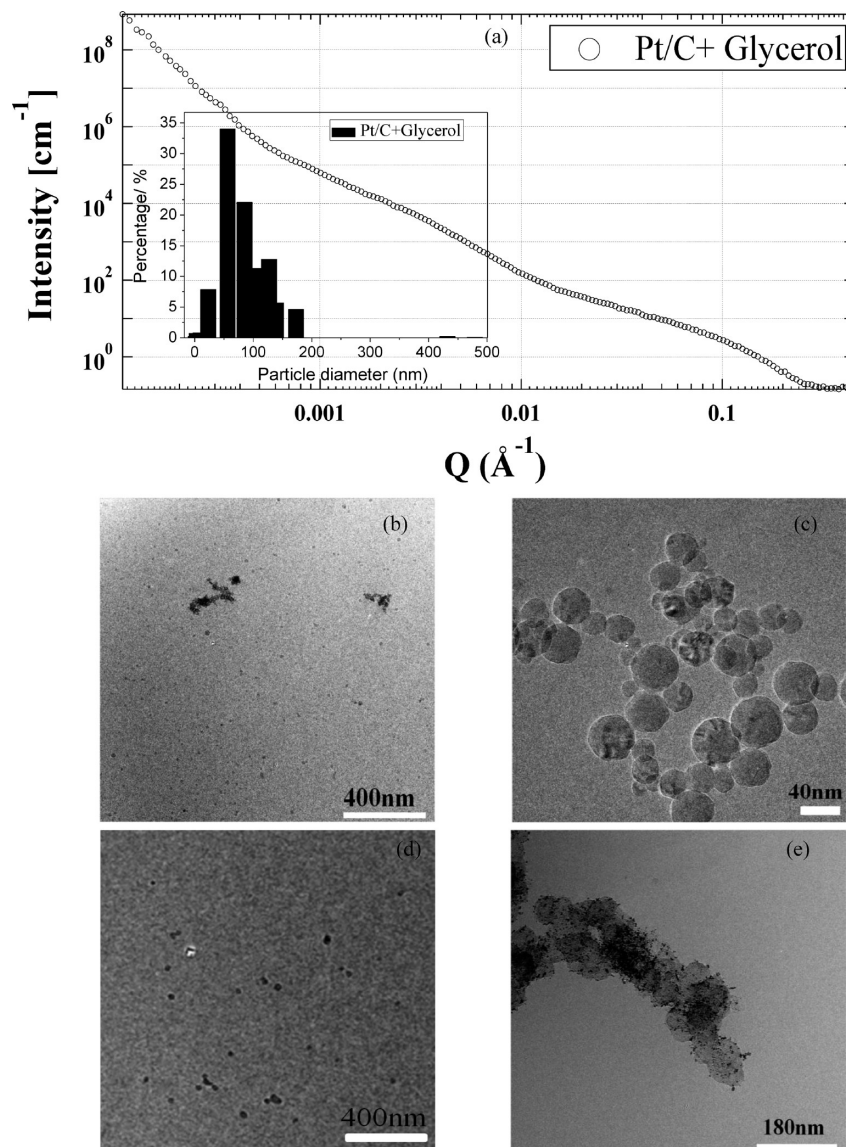


Figure 5. (a) USAXS plots of the 28% Pt/C + glycerol solution with the particle size distribution. (b) Overview of cryo-TEM images of different particles in the sample. (c) Cryo-TEM image corresponding to the first-level fitting. (d) Cryo-TEM image corresponding to the second-level fitting. (e) Cryo-TEM image corresponding to the third-level fitting.

unified fitting levels ($n = 4$) were employed in the global unified function fitting for the scattering data of the Pt/C + Nafion system. The corresponding geometries of the particles from the cryo-TEM images were inserted in the different levels. As can be seen from Figure 6 (Pt/C + Nafion), the high- q regime from 0.1 to 1 \AA^{-1} was assigned to the first level, as shown in Figure 6b, which started with the first Porod fit and was followed by the first Guinier fit. The fitting results showed a power-law slope of $P_1 = 1.5$ and $D_{g_1} = 3.9 \pm 0.2 \text{ nm}$, which are consistent with the Nafion ionomer size shown in the cryo-TEM. Therefore, level one can be attributed to the Nafion ionomer rodlike particles with a diameter of about $4.2 \pm 0.2 \text{ nm}$, as shown in the inset TEM image. The second-level fitting (Figure 6c) was carried out from 0.01 to 0.1 \AA^{-1} , resulting in $D_{g_2} = 66 \pm 1.4 \text{ nm}$ and power-law slope of $P_2 = 2.7$. According to the cryo-TEM image, the diameter of a single carbon particle, which had spherelike geometry, was close to $70 \pm 5 \text{ nm}$, which is very close to the USAXS second-level fitting results. In the medium- q part in Figure 6d, from 0.001 to 0.01 \AA^{-1} , the third-level fitting results were in the particle size range of about $D_{g_3} = 205.4 \pm 10 \text{ nm}$ with a power-law slope of

$P_3 = 3.4$, which indicates aggregated particles in the system. The aggregated particles can be observed in the cryo-TEM image inset in Figure 6d, where four to five carbon spheres aggregated to form one large rodlike particle whose diameter was $\sim 60 \pm 2 \text{ nm}$ and whose length was $\sim 150 \pm 10 \text{ nm}$. As can be seen from the fourth level (from 0.0001 to 0.001 \AA^{-1} in Figure 6e), $D_{g_4} = 292.3 \pm 5 \text{ nm}$ and the power-law slope is $P_4 = 4$. The corresponding cryo-TEM image in the level-four fitting in Figure 6a shows an L-shaped aggregated particle with a length of $\sim 200 \text{ nm}$.

Overall, the Pt/carbon + Nafion solution appears to be a complex multiparticle system with different particle sizes and geometries. The primary particle size distribution was obtained from USAXS with Igor software after normalization. Some of the Nafion ionomer rodlike particles wrapped around the Pt/C particles (cryo-TEM image in Figure 6e) but not all Pt/C particles were surrounded by Nafion particles (cryo-TEM images in Figure 6c,d). On the basis of the USAXS data, according to the unified global fitting (to determine the fitting level) and cryo-TEM images (geometry information), four levels were employed in the particle size distribution analysis from high q to low q ,

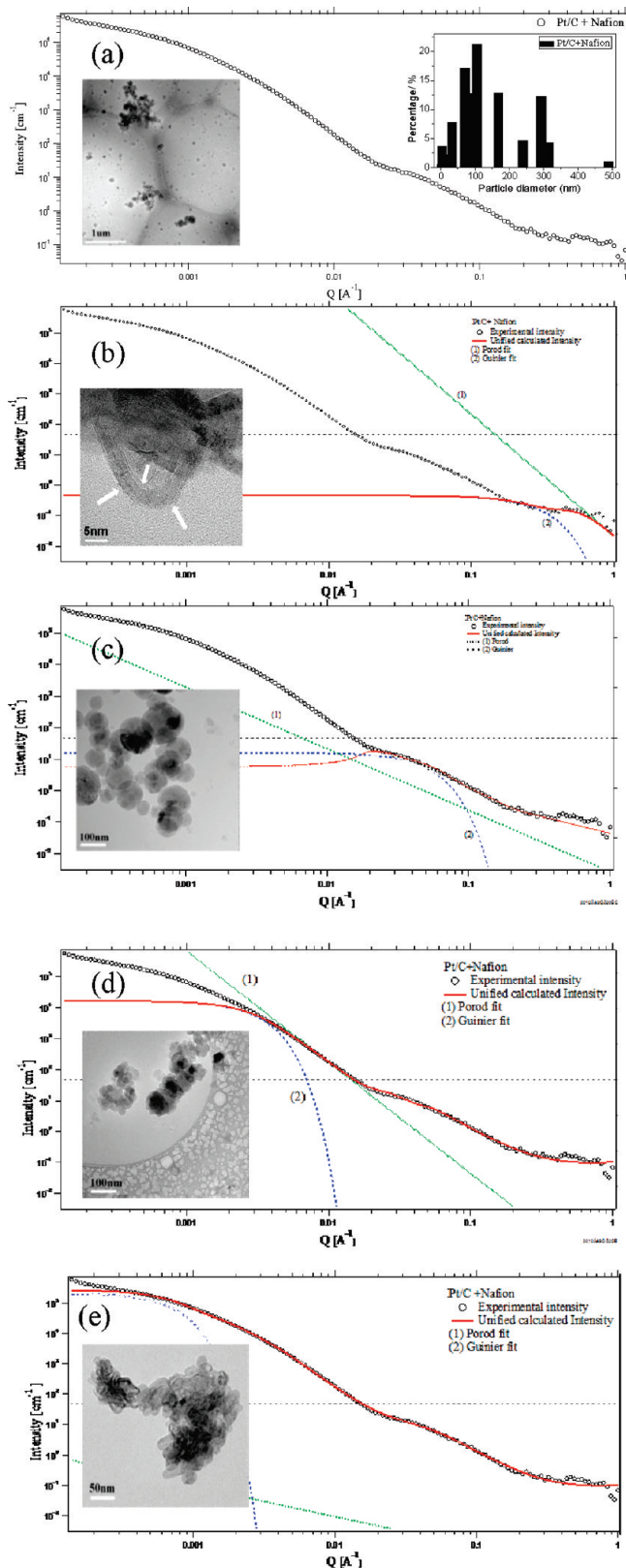


Figure 6. USAXS plots of a 28% Pt/C + Nafion solution, step-by-step fitting from a high- q region to a low- q region, and cryo-TEM images of different particles in the sample with the size distribution. (a) Overview cryo-TEM image corresponding to whole USAXS fitting. (b) Cryo-TEM image corresponding to first-level fitting. (c) Cryo-TEM image corresponding to second-level fitting. (d) Cryo-TEM image corresponding to third-level fitting. (e) Cryo-TEM image corresponding to fourth-level fitting.

which was similar to the unified global fitting process. The MaxEnt method was used in all levels of analysis. On the basis of the analysis shown above, the first level was attributed to the Nafion ionomer; therefore, from the Nafion ionomer geometry and particle size information obtained in a previous section, a cylinder model with a length of 15 nm was set in the first level. In a similar approach, a spheroid model was employed in the second level. Then another two cylinder models with lengths of 100 and 150 nm were used in the third and fourth levels, respectively. The full-range particle size distribution is the inset of Figure 6a, in which a primary particle diameter of $\sim 60\text{--}100$ nm could be obtained. According to the overview cryo-TEM image inset in Figure 6a, it can be seen that the primary particles were the spherelike carbon particles with a diameter of $\sim 70\text{--}100$ nm. The results from the two technologies matched each other very well.

Pt/Carbon Black + Nafion + TBAOH System. Nafion ionomer particle growth caused by TBAOH has been discussed in the previous section (Nafion + TBAOH system). The Pt/carbon black + Nafion + TBAOH system was also investigated. Again, this system had nonuniform particle sizes and geometries and required multilevel fitting. The USAXS results are shown in Figure 7. Using the same data-fitting approach as in the above discussion, the fitting results showed $D_{g_1} = 3.6 \pm 0.2$ nm with a power-law slope of $P_1 = 1.21$ in the first fitting level. According to the Pt/C + Nafion system and on the basis of previous results, it can be concluded that this fitting level can be attributed to the Nafion ionomer particles, as the cryo-TEM image (Figure 7c) shows. The second fitting level was $D_{g_2} = 64 \pm 4$ nm (with a power-law slope of $P_2 = 2.74$), which can be confirmed by the cryo-TEM image (Figure 7c). From 0.001 to 0.01 \AA^{-1} , a third fitting level, $D_{g_3} = 201.7 \pm 10$ nm, and a power-law slope, $P_3 = 2.63$, were obtained and resulted in an aggregated rodlike particle with a length of ~ 100 to 250 nm, as shown in the cryo-TEM image (Figure 7d). The fourth-level fitting was employed to fit the low- q area. These fitting results showed $D_{g_4} > 300$ nm and a power-law slope of $P_4 = 2.77$. In the cryo-TEM image (Figure 7f), a larger aggregated particle formed that was 420 nm. The full-range particle size distribution based on the USAXS data obtained by a similar process as in the Pt/C + Nafion system is shown in Figure 7. The primary particle size in this system was about 120 to 200 nm (contribution from aggregated carbon particles), which is much higher than that of the Pt/C + Nafion system (70–100 nm). The overview TEM image (700 nm, Figure 7d) shows that the primary particle size in this system of aggregated carbon particles was about 200 nm, which confirms the USAXS data. The increased particle size might be caused by the TBAOH effect.

Pt/C + Nafion Ionomer + Glycerol System. As for the Pt/C + Nafion ionomer + glycerol system, the scattering data and cryo-TEM images are shown in Figure 8. With the same fitting protocol, the fitting results showed $D_{g_1} = 3.2 \pm 0.4$ nm with a power-law slope of $P_1 = 1.5$ in the first fitting level, which can be attributed to the Nafion ionomer particle. From 0.01 to 0.1 \AA^{-1} , the second fitting level was employed to get $D_{g_2} = 54 \pm 2$ nm with $P_2 = 3.31$. Similar to the above-mentioned Pt/C + Nafion + TBAOH system (Figure 7c), a spherelike carbon particle was observed in the cryo-TEM image (Figure 8c), indicating that this level was dominated by single spherical particles. Another level was used to fit the lower- q region. A power-law slope of $P_3 = 3.38$ and $D_{g_3} = 159.7 \pm 10$ nm was obtained. From the corresponding cryo-TEM image (Figure 8d), this level can be attributed to the rodlike carbon particles. About 20 spherical carbon particles ($D = \sim 30$ nm) aggregated to form the rodlike particles (length = 350 nm, width = ~ 90 nm). The lowest q region was fit to get $D_{g_4} = 290 \pm 10$ nm with a power-law slope of $P_4 = 2.68$, which is

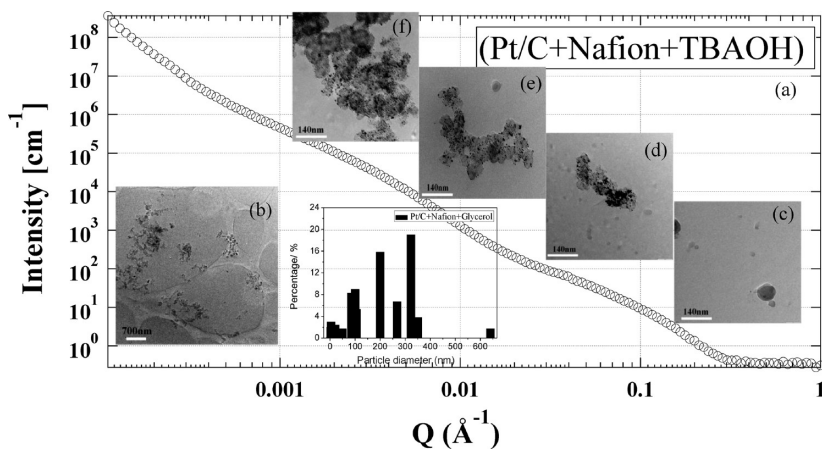


Figure 7. (a) USAXS plots of the 28% Pt/C + Nafion + TBAOH solution and particle size distribution. (b) Overview of cryo-TEM images of different particles in the sample corresponding to whole USAXS fitting. (c) Cryo-TEM image corresponding to second-level fitting. (d) Cryo-TEM image corresponding to third-level fitting. (e, f) Cryo-TEM images corresponding to fourth-level fitting.

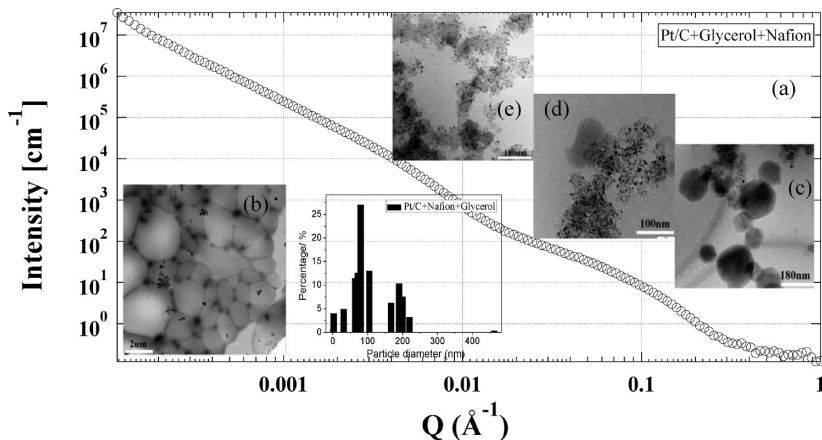


Figure 8. (a) USAXS plots of the 28% Pt/C + glycerol + Nafion solution and particle size distribution. (b) Overview of cryo-TEM images of different particles in the sample. (c) Cryo-TEM image corresponding to the second-level fitting. (d) Cryo-TEM image corresponding to the third-level fitting. (e) Cryo-TEM image corresponding to the fourth-level fitting.

consistent with the agglomerated particles in the TEM image (Figure 8e). As can be seen from the TEM image (Figure 8e), it was found that the carbon rods connected to form a net-shaped particle whose length could reach about 500 nm or longer. The particle size distribution was inserted in Figure 8, which was obtained by the four-level analysis mentioned previously. The full-range particle size distribution is the inset in Figure 8, where the primary particle size for the Pt/C + Nafion + glycerol system is 90 nm. From the overview TEM image (Figure 8b), it can be observed that the primary particle was the aggregated rodlike particle with a particle size of about 80 nm. Two results suggest that the carbon spherical particle composed of three or four monocarbon particles was the dominating particle in this system. Furthermore, the percentage of particles with a diameter of about 72 ± 5 nm is smaller than that in the Pt/C + glycerol system yet larger than that in the Pt/C + Nafion system. (See the particle size distributions in each system.) The percentage of the particles with ~ 60 nm diameter was about 41% for the Pt/C + glycerol system, 17.4% for the Pt/C + Nafion system, and 24% for the Pt/C + Nafion + glycerol system, respectively, indicating that glycerol could greatly improve Pt/C and Nafion ionomer particle dispersions and that the Nafion ionomer may cover/bind the carbon black particles to form a larger particle. (A new approach has been designed to provide cryo-TEM images showing the Nafion

ionomer with Pt/C. A detailed investigation of the Pt/C and Nafion interaction will be reported in our next publication.)

Twenty-Eight Percent Ink System (Pt/C + Nafion + TBAOH + Glycerol). The 28% ink is typically used to make the catalyst layer/MEA, which leads to the Nafion content in a solid catalyst layer being 28 wt %. The detailed ink composition for this system is shown in Table 1. On the basis of the results above, it can be deduced that the catalyst ink system includes monoparticle systems (Pt/carbon, Nafion ionomer), aggregated particle systems (Pt/carbon aggregated particles and Nafion/carbon aggregated particles), and agglomerated particle systems, which are also shown in the overall cryo-TEM image (Figure 9b). The USAXS data and TEM images of the 28% ink (Pt/C + Nafion + TBAOH + glycerol) are shown in Figure 9. The four levels of fittings were also used for this sample. The first fitting level attributed to the Nafion ionomer particles had a diameter of about 3.28 ± 0.4 nm and a power-law slope of $P_1 = 3$. The porod slope was a little higher than before (1.2–2), which might be caused by the geometry change of the Nafion ionomer; however, it is still hard to see the Nafion ionomer structure in the cryo-TEM image (Figure 9c). Other work has been carried out to investigate the detailed geometrical structure of the Nafion ionomer in the catalyst ink. A particle size of $D_{g_2} = 47.4 \pm 2.5$ nm with a power-law slope of $P_2 = 3.3$ was obtained from the second-level fitting.

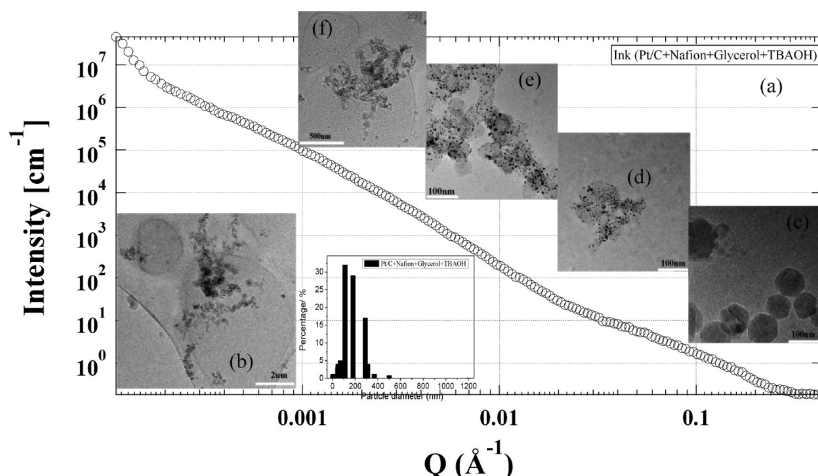


Figure 9. (a) USAXS plots of the 28% catalyst ink solution and particle size distribution. (b) Overview of cryo-TEM images of different particles in the sample. (c) Cryo-TEM image corresponding to the second-level fitting. (d) Cryo-TEM image corresponding to the third-level fitting. (e, f) Cryo-TEM images corresponding to the fourth-level fitting.

The single carbon spherical particle with a diameter equal to about 50 nm can be seen in the cryo-TEM image (Figure 9d). On the basis of the particle size distribution inset in Figure 9, the percentage of single carbon spherical particles (diameter = 50 nm) was about 12%, which is similar to that in the Pt/C + Nafion + TBAOH system. The percentage of particles around 100 nm of about 30% was also obtained from the particle size distribution, which might be from the contribution of two single carbon spherelike particles. In the cryo-TEM image in Figure 9e, there are aggregated carbon particles (200 nm × 250 nm) composed of about 21 small, single carbon particles ($D = 25$ nm), which is consistent with the third-level fitting results of $D_{g_3} = 169.8 \pm 10$ nm with a power-law slope of $P_3 = 3.19$. In the fourth fitting level, a large particle with $D_{g_4} = 290 \pm 10$ nm and a power-law slope of $P_4 = 4$ was found. The geometry was also obtained from the cryo-TEM image (Figure 9f), which showed 50–60 single carbon spherical particles composed of a 600 nm × 500 nm agglomerated particle. The primary particle size obtained from both the USAXS particle size distribution result and the cryo-TEM results was between 100 and 200 nm. Overall, because of the interactions of Pt/C, Nafion and TBAOH, glycerol, the particles in the catalyst ink system are not uniform in size; rather, a wide range of particle sizes with different geometries is seen in the distribution. Moreover, the particles in the ink system form a hierarchical structure (as schematically shown in Figure 3 in the Supporting Information) in which primary particles form aggregates and aggregates form agglomerates.

5. Conclusions

USAXS has been successfully used to study the microstructural organization of Nafion ionomer particles and Pt/C aggregates dispersed in liquid media. Careful, sophisticated data analysis, namely, multiple curve fittings, was required to interpret/extract the correct results from the scattering data. The cryogenic TEM analysis helped to validate the USAXS results, by which the size and geometry of the Nafion ionomer particles and Pt/C aggregates dispersed in liquid media were directly observed. The results

from these two techniques, cryogenic TEM and USAXS, show excellent agreement, suggesting that USAXS can be used as a powerful, accurate, and easy tool for studying catalyst ink dispersion and, consequently, for validating the ink formulation. This systematic, comprehensive study shows that the dispersion of each component (i.e., Pt/C particles and Nafion particles) in liquid media is different and that the solvents (glycerol and isopropanol) have different effects on Pt/C and Nafion ionomer dispersions. The USAXS data show that the agglomerate size of the catalyst and the Nafion ionomer particle size changed significantly with different ink compositions, suggesting that interactions between each component exist. The TEM image shows that the catalyst ink was composed of a Nafion ionomer with rodlike particles ($D = 3$ nm, $L = 20$ nm), single spherical carbon black particles ($D = \sim 30$ –70 nm), rodlike aggregated carbon black particles ($D = 300$ nm), and some much larger aggregate particles ($D > 400$ nm). The geometry and size of each system of Nafion ionomer particles and Pt/C aggregates are not uniformly distributed; rather, they vary significantly. This work also demonstrates that the size and geometry of a nonuniform system can be studied with USAXS. Further work on the interaction of each component is underway and will be reported in the near future.

Acknowledgment. We express our appreciation to the Advanced Photon Source, Argonne National Laboratory, for providing the access to the USAXS beamline and the National Institute of Standards and Technology (NIST) for providing the access to the SANS and USANS beamlines. Without such access, this work could not be completed. We also thank Dr. Yuan Liu of NIST for helpful discussions on these scattering techniques and data processing.

Supporting Information Available: Typical scheme of the MEA structure. Experimental process. Hierarchical structure. This material is available free of charge via the Internet at <http://pubs.acs.org>.